Forestry Advance Access published March 17, 2009

Carbon stock and stock changes across a Sitka spruce chronosequence on surface-water gley soils

KEVIN BLACK[1,2]*, KENNETH A. BYRNE[3], MAURIZIO MENCUCCINI[4], BRIAN TOBIN[2], MAARTEN NIEUWENHUIS[2], BRIAN REIDY[2], TOM BOLGER[2], GUSTAVO SAIZ[2], CARLY GREEN[2], EDWARD T. FARRELL[2] AND BRUCE OSBORNE[2]

[1] Forest Environmental Research and Services (FERS Ltd), Ard Brae Court, Vevay Road, Bray, Co. Wicklow, Ireland
[2] School of Biology and Environmental Science, University College Dublin, Belfield, Dublin 4, Ireland
[3] Department of Life Sciences, University of Limerick, Limerick, Ireland
[4] School of GeoSciences (IERM), Edinburgh University, Crew Building, West Mains Road, Edinburgh EH9 3JN, Scotland
*Corresponding author. E-mail: kevin.black@ucd.ie

Summary

We assessed age-related alterations in carbon (C) stocks and sequestration rates of first rotation Sitka spruce (*Picea sitchensis* (Bong.) Carr) plantations on predominantly surface-water gley soils. Sites were selected to represent a typical Sitka spruce chronosequence following land use transition from grasslands dominated by surface-water gley soils. Based on inventory, eddy covariance, physiological and modelling assessments of net ecosystem productivity (NEP), we show that afforested stands are a C sink at 10 years, and possibly earlier, followed by an increase to a maximum of 9 t C ha^{-1} $year^{-1}$ before the first thinning cycle. NEP subsequently declined from 9 t C ha^{-1} $year^{-1}$, at closed canopy, to 2 t C ha^{-1} $year^{-1}$ in older and thinned stands. Reductions in the C sequestration rate of older stands were coupled with a decrease in gross primary productivity, increases in maintenance/growth respiration and decomposition losses following harvest. We suggest that the high sequestration potential of these forests may be associated with the high net primary productivity of these plantations in Ireland, a high allocation of assimilates and litter into the belowground C pool and accumulation of C in mineral gley soils following afforestation.

Introduction

Newly planted forests offer the potential to offset CO_2 emissions by taking up and storing carbon (C) in forest biomass and soils. The sequestration potential of these forest sinks in Ireland has been substantially enhanced by the establishment of more than 250 000 ha of plantation forest since 1990, most of which (~50 per cent) is pure Sitka spruce stands. While historically most afforestation has taken place on peat soils, increased plantation establishment on marginal grasslands, primarily on surface-water gleys, has resulted in a proportional decline in the afforestation of peat soils from 56 per cent in 1990 to 29 per cent in 2003. Clearly, therefore, more information on

Sitka spruce forests occurring on mineral soils is required in order to provide a better understanding of the C-sequestrating capacity of recently planted forests in Ireland. Although the establishment of forest plantations on mineral soils offers the potential to sequester C over the short to long term, the magnitude of the forests sink varies considerably with stand age (Waring *et al.*, 1998; Kolari *et al.*, 2004; Kowalski *et al.*, 2004; Magnani *et al.*, 2007).

Net ecosystem productivity (NEP) represents the C balance resulting from C losses (sources) due to disturbance and decomposition and C gains (sinks) due to stand photosynthesis (gross primary productivity, GPP) and growth (net primary productivity, NPP). The forest ecosystem is typically a C source over the first few years, followed by a net uptake and peak in NEP prior to canopy closure. In older stands, NEP declines due to higher decomposition losses associated with thinning and accumulated litter, lower GPP by the trees and lower leaf area index (LAI, Waring *et al.*, 1998). The dynamics associated with the transition from a source to a sink and the timing of the decline in older stands is dependent on numerous factors including management, soil type, species, productivity and climatic conditions. The magnitude of the variations in age-related dynamics makes it difficult to understand the controlling processes and the magnitude of forest sinks at the regional and global scale.

In this study, we report on the changes in total C stocks and component C fluxes of a Sitka spruce chronosequence located on surface-water gley soils using a combination of eddy covariance, traditional inventory, physiological information and modelling. We discuss the factors contributing to and the magnitude of the sequestration potential of this forest type in Ireland in relation to global and European temperate coniferous forests.

Methodology

Site description and management

A chronosequence of eight, even-aged, first rotation, Sitka spruce stands of typical Yield Class (YC) (a productivity index based on top height and stand age (YC) = 20–24) and management regimes, with similar edaphic and climatic conditions, extending across a typical rotation length in Ireland were identified (Tables 1 and 2). The age classes of the selected stands across the chronosequence were normalized to 22, based on top height to age functions according to Edwards and Christie (1981, see Table 2). Site D14 was selected as the core site, where eddy covariance measurements were made and the information obtained from this site used to parameterize ecosystem models. Standard measurements that were made at all sites included inventory surveys, soil C analysis, soil respiration measurements, litter fall collections and biomass harvests.

The land use prior to afforestation was rough grassland or pasture (predominantly *Agrostis spp*, *Holcus lanatus* L. and *Lolium perenne* L.) with *Carex pauciflora* Lightf., *Ulex gallii* L. and *Rubus fruticosus* agg. encroaching from drains and hedgerows (Table 1 and 2). Cultivation at establishment was either mole drained, mouldboard ploughed or ripped drains (Table 1). Planting on the younger sites (B9, D9, C14 and D14) was along ripped lines, 1 m deep and 2 m apart. Surface drains were installed at right angles to the cultivation lines at 50-m intervals. Prior to establishment, the older sites (G24, D30, C45 and D47) were ploughed at 1.7-m intervals, following the contour lines of the slope. No fertilizer was applied at or after establishment.

Soil descriptions

Stands established on surface-water gley soils were chosen as a representative of mineral soil sites supporting post-1990 plantations of Sitka spruce in Ireland. The soil type and texture was similar for all the selected stands. However, the water-holding capacity of the soil in the C45 stand was lower due, most probably, to increased surface runoff resulting from the 10 per cent slope. Mean sand, silt and clay contents of the sites in the chronosequence were 22 , 36 and 42 per cent, respectively (Table 3).

Biomass harvests

The data used for the development of total biomass and biomass component models (Table 4) were based on trees harvested in 2003 (see Tobin *et al.*, 2006). Prior to harvesting, the height, top height and diameter at breast height (d.b.h.) of all trees in three randomly located plots at each site (~100 individuals) were measured for estimation on YC

Table 1: Location and management history of chronosequence sites

Site name/code	Planting date	YC	Georeference position	Previous land management	Cultivation and management	Thinning history (dates)
Baunoge (B9)	1993	22	52° 55′ N, 7° 14′ W	Grass/rush pasture	Ripped (1 m depth with ball and chain), surface drains across rip lines, no fertilizer	not applicable
Dooary (D9)	1993	22	52° 57′ N, 7° 15′ W	Grass/rush pasture	Ripped (1 m depth with ball and chain), surface drains across rip lines, no fertilizer	not applicable
Clontycoe (C14)	1988	22	52° 56′ N, 7° 15′ W	Poor fertilized marginal grassland	Ripped (1 m depth with ball and chain), surface drains across rip lines, no fertilizer	not applicable
Dooary (D14)	1988	24	52° 57′ N, 7° 15′ W	Grassland, regularly fertilized	Ripped (1 m depth with ball and chain), surface drains across rip lines, no fertilizer	Due in 2007
Glenbarrow (G24)	1978	20	53° 8′ N, 7° 27′ W	Rough grassland	Mouldboard ploughed, poor establishment (80%)	First 1998
Dooary (D30)	1972	22	52° 57′ N, 7° 16′ W	Grass pasture	Mole drained, shallow ploughed, no fertilizer	1991, 1995, 1999, 1903
Cullenagh (C45)	1957	22	52° 57′ N, 7° 15′ W	Rough grassland	Mouldboard ploughed, no fertilizer	Mid-1970s, 1981, late 1980s, mid-1990s, 2001 and felled in 2004
Dooary (D47)	1955	22	52° 57′ N, 7° 16′ W	Grass pasture	Mouldboard ploughed, no fertilizer	Mid-1970s, 1981, late 1980s, mid-1990s, 2001 and felled in 2003.

(Table 2) and other model parameters (see Appendix 1). C and nitrogen (N) contents of the dried biomass samples were measured using a C–N analyser (Leco CSN-1000, Leco Corp., St Joseph, MI, USA).

Estimates of specific leaf area and LAI were taken from a related paper (Tobin *et al.*, 2006).

Fine root biomass and turnover data were derived from published estimates previously reported for the same sites (Saiz *et al.*, 2006, 2007; Black *et al.*, 2007).

Annual surveys

Four randomly selected sampling plots at each site within the chronosequence (Table 2) were surveyed over a period of 1 week in July 2002 to obtain inventory information including tree height, height to crown base, crown diameter and d.b.h. measurements. Plots were of 0.01 ha size at sites B9, C14 and D14. This was increased to 0.02 ha at the G24 and D30 stands and 0.03 ha at the C45 stand, in order to account for the lower number of trees per hectare in the older stands. This ensured that between 20 and 35 trees were measured in each plot. In 2002, the trees were marked with white paint at 1.3 m high (i.e. at breast height) so that the d.b.h. measurements could be repeated in 2004 at the same points. Tree height was estimated using a laser hypsometer (Laser Technology Inc., Centennial, Colorado).

Litter and soil analysis

Litter input was measured monthly using 35 cm diameter collectors (n = 10) at each site. For the grassland site (G0), litter fall estimates were made

Table 2: Description and stand characteristics of chronosequence stands in 2002

Forest code	Rescaled age* (Years)	Stocking density (stem ha^{-1})	d.b.h. (cm)	Height	Basal area (m^2 ha^{-1})	LAI† (m^2 m^{-2})	Crown to height ratio
B9	9	2333	6	3.5	6.3	4.3	0.08
C14	14	2533	13	7.3	34.0	7.2	0.13
D14	16	2467	16	9.5	52.2	7.4	0.41
G24	22	1250	22	14.3	48.9	5.7	0.56
D30	30	1033	24	16.8	60.7	5.6	0.59
C45	45	767	31	24.7	65.3	4.8	0.62
D47	47	821	33	26.5	70.2	n.d.	0.61

n.d. = not determined.
* Stand ages were normalized to a YC of 22 based on top height–age functions (Edwards and Christie, 1981).
† LAIs of stands were previously reported by Tobin *et al.* (2006).

Table 3: Soil description and characteristics of sites where soils were sampled and soil respiration measurements were taken

Forest code	Rescaled age (years)*	Sand (%)	Silt (%)	Clay (%)	pH	Topography/ slope (%)	Bulk density (kg m^{-3})
G0	0	23	41	36	5.3	3	0.918
B9	9	37	32	30	4.8	1	0.950
D14	16	9	38	53	5.0	3	0.998
D30	30	14	39	47	4.3	8	1.002
C45	45	20	50	30	4.3	10	1.063
D47	47	n.d.	n.d.	n.d.	4.1	4	1.054

* Stand ages were normalized to a YC of 22 based on top height–age curves (Edwards and Christie, 1981).

Table 4: Regression models for total biomass (TB) and biomass C partitioning into stem (St_f), timber (stem up to diameter > 7 cm; T_f), coarse root (>5 mm; CR_f), needle (N_f), live branch (B_f) and attached dead branch (DB_f) fractions expressed as a ratio of total tree biomass C (TB, excluding fine root biomass < 5 mm)

Biomass fraction	Model	r^2	SEE
TB	$0.286 \times (\text{d.b.h.} \times H)^{1.138}$	0.98	0.021
St_f	$0.2814 + 0.4346 \times (1 - \exp(-0.0089 \times TB))$	0.92	0.057
T_f	$-0.0128 + 0.654 \times (1 - \exp(-0.0139 \times TB))$	0.96	0.052
CR_f	$0.1571 + 0.1396 \times \exp(-0.0079 \times TB)$	0.79	0.041
N_f	$0.0332 + 0.18 \times \exp(-0.0178 \times TB)$	0.95	0.016
B_f	$0.0459 + 0.2438 \times \exp(-0.019 \times TB)$	0.96	0.02
DB_f	$-0.0119 + 0.1099 \times \exp(-0.5 \times (\text{Ln}(TB/159.88)/1.0558)^2)$	0.84	0.023

Regression models are based on a sample of 36 trees from stands shown in Table 2 (six trees per site). The St_f and T_f functions include bark biomass.
SEE = standard error of estimates.

using the harvest technique of Sims *et al.* (1978). The same technique was also used to estimate the increase in grass litter due to canopy closure in the 9-year-old site (D9). The green leaf and bud scale components of litter fall (ΔF_{litter}) were used in the NPP estimates (see Black *et al.*, 2007). The C and N concentrations were measured using a CHN analyser.

A total of 15 soil cores per site (10 cm diameter with a penetration depth of 30 cm including the O, A, B and E horizons) were collected over an area of 900 m^2 during the 2003–2004 season. Total C content of the soils at each site was estimated for each of the organic and upper mineral horizons based on loss on ignition, which was calibrated using a CHN analyser. The soil C stock in the top 30 cm of the mineral layer was calculated using C content and bulk density of the soil core (for detailed procedure see Black and Farrell, 2006).

Soil respiration, harvest residue and decomposition

Soil respiration measurements at four sites (D9, D14, D30 and C45), as reported by Saiz *et al.* (2006, 2007), allowed the investigation of autotrophic and heterotrophic components to soil respiratory flux.

Estimates of harvest residue (Hr) in the form of stumps and dead wood >7 cm diameter were taken from published data obtained from the same experimental sites (see Tobin *et al.*, 2007).

The decomposition of dead branches and needles still attached to trees (Br) was calculated according to Black *et al.* (2007).

Parameterization of MAESTRA

MAESTRA (http://www.bio.mq.edu.au/maestra/), a modified version of MAESTRO (see Norman and Jarvis, 1974, 1975; Wang and Jarvis, 1990a, b), is a light interception and photosynthesis model representing an array of trees in a stand. The model comprises seven submodels, which account for the radiation absorbed by leaves and CO_2 and water exchanges between leaves in the crown and the ambient air. MAESTRA differs from other models because it takes account of the heterogeneous distribution and age structure of leaves within the canopy. These structural characteristics are important for estimating radiation absorption and GPP of a conifer canopy (Wang and Jarvis, 1990b).

The inputs to the submodels include site, soil, leaf, physiological, tree, weather and radiation data. Details of specific parameters are included in Appendix 1. The site information relating to geographical reference, plot dimensions and trees per plot were obtained from the same chronosequence plots surveyed in 2002 (Tables 1 and 2). The x, y and z coordinates, crown radii, live crown length, heights and total leaf area were obtained from measurements taken in the 2002 survey, supplemented by measurements made in early 2003 and published data from the same plots (Black *et al.*, 2004; Black and Farrell, 2006; Tobin *et al.*, 2006, 2007).

The physiological parameters were taken from the literature (Appendix 1). Leaf N concentration was obtained from harvested tree data obtained in 2003 at sites specified in Tables 1 and 2.

An automatic weather station installed at the D14 (Campbell Scientific Ltd, Shepshed, England) recorded meteorological data, including air temperature, relative humidity, wind speed above the canopy and direction, net radiation, incident irradiance, the diffuse fraction of irradiance, air pressure and rainfall. The ambient CO_2 concentration was assumed to be 380 μmol mol^{-1}.

Validation of GPP output from MAESTRA

Eddy covariance measurements of net ecosystem exchange (NEE ≈NEP) were made over the period from February 2002 to February 2004, as described in detail by Black *et al.* (2007). GPP outputs from MAESTRA for the D14 stand were validated using GPP estimates derived from eddy covariance assessments (Black *et al.*, 2006):

$$\mathrm{GPP} = -\mathrm{NEE} - \mathrm{Rd}, \quad (1)$$

where NEE is net ecosystem exchange and Rd is annual respiration (t C ha^{-1} $year^{-1}$). For a detailed description of the eddy covariance-based estimates of GPP refer to Black *et al.* (2006). GPP estimates were validated for the D14 stand only.

Calculation of ecosystem C balance

It was not possible to derive eddy covariance-based estimates of NEP across the chronosequence due to logistical and budgetary constraints. Therefore, NEP was derived from assessments of NPP and annual estimates of ecosystem heterotrophic respiration (Rh). However, NEP could not be estimated for all stands in the chronosequence due to

the lack of respiration data required to close the C balance from the C14 and G24 stands (Table 1). Where possible, NEP was calculated as

$$\mathrm{NEP} = \mathrm{NPP} - \mathrm{Rh} \quad (2)$$

with

$$\mathrm{Rh} = \mathrm{Fs}_{\mathrm{het}} + \mathrm{Hr} + \mathrm{Br}. \quad (3)$$

NPP was estimated from inventory data using the approach adopted by Black *et al.* (2007). Decomposition losses are the sum of heterotrophic respiratory fluxes associated with soils and litter ($\mathrm{Fs}_{\mathrm{het}}$, Saiz *et al.*, 2006), harvest residues (Hr) and dead branches attached to the tree (Br, Black *et al.*, 2007; Tobin *et al.*, 2007).

For the purpose of compiling a complete C balance, autotrophic respiration (Ra) was derived as the difference between GPP and NPP estimates.

Belowground C allocation

Total belowground C allocation (TBCA) was estimated using the mass balance approach as described by Giardina and Ryan (2002), where inputs into the system are assumed to be equal to outputs over a period of time (Zerva *et al.*, 2005):

$$\mathrm{TBCA} = \mathrm{Fs}_{\mathrm{tot}} + \mathrm{Fe} - \Delta\mathrm{Litter} + \Delta\mathrm{SOM} + (\Delta\mathrm{Fr} + \Delta\mathrm{Cr})/\Delta t. \quad (4)$$

Values for $\mathrm{Fs}_{\mathrm{tot}}$, the total soil respiration, were taken from Saiz *et al.* (2006); Fe, the flux of C due to leaching, runoff and erosion, was assumed to be of minor significance (Zerva *et al.*, 2005); ΔLitter, the total litter fall was taken from Tobin *et al.* (2006); ΔSOM, the soil stock change, was assumed to be represented by the difference in soil C stock over the chronosequence; ΔFr, fine root turnover, was taken from Saiz *et al.* (2006) and ΔCr, the coarse root (>5 mm diameter) increment, was estimated using repeat inventory measurements and biomass algorithms (Table 4). All fluxes were calculated as t C ha^{-1} year^{-1}.

Statistical analysis

We examined potential uncertainties associated with the sampling, model and measurement errors for the different ecosystem component estimates. Sampling errors, in this case, represent the variability in the estimate due to measuring a subset of the population. Model errors, such as the allometric functions or respiration models, were estimated using per cent SEE from regression analysis of observed and predicted values (see Black *et al.*, 2007). The only measurement errors assessed were the tolerances for d.b.h. (1 mm) and height (0.05 m). The total combined standard error for all components was estimated as:

$$\sigma_x = \sqrt{\sigma_a^2 + \sigma_b^2 + \sigma_c^2 + \sigma_{n+1}^2} \quad (5)$$

where, σ_x is the total standard error and σ is the standard error of individual components.

Results

Biomass C stocks and allocation

The biomass C stock of the non-forested grassland site was estimated to be 2.3 t C ha^{-1}. Standing biomass C stocks of afforested stands varied from 14.1 t C ha^{-1}, for the 9-year-old stand, to 211 t C ha^{-1}, for the 45-year-old stand (Table 5). The biomass stock removed from the stands subjected to thinning (i.e. G24, D30, C45 and D47) varied from 29.6–132.7 t C ha^{-1} depending on stand age and number of thinning cycles. The harvest residue C stock resulting from cut stumps and logs accumulating on-site after harvest was 4.9 t C ha^{-1} after the first thinning cycle (i.e. site G24) and ~26 t C ha^{-1} for sites (D30 and C45) subjected to two or more thinning cycles (Table 5).

The relative allocation of biomass into timber, as evident from the ratio of total biomass to timber biomass (i.e. biomass expansion factor, BEF), varied from 12.8 to 3 t t^{-1} in the younger stands prior to the first thinning. Biomass allocation into timber increased after stands were thinned and remained constant (BEF ~ 1.6 t t^{-1}) in the older stands (30–47 years old, Figure 1A). The increased allocation into timber across the chronosequence was consistent with an increased allocation into aboveground relative to belowground biomass (S : R; Figure 1A, Table 5). The aboveground biomass allocation into live needles and branches (used here as a proxy measure of photosynthetic tissue) generally increased with stand age. However, the allocation into the photosynthetic,

Table 5: Biomass component stock and stock changes over the chronosequence

	Stand age*							
	0	9	14	16	22	30	45	47
C pool stocks (t C ha^{-1})								
Stems		3.5 ± 1.9	15.5 ± 6.2	27.3 ± 2.3	74.2 ± 16.4	95.9 ± 13.5	151.9 ± 2.8	105.8 ± 8.6
Timber		1.1 ± 0.8	10.4 ± 5.7	20.9 ± 2.4	68.5 ± 15.2	88.1 ± 12.5	136.7 ± 1.7	95.9 ± 7.9
Live needles		1.8 ± 0.7	4.3 ± 0.8	5.8 ± 0.3	4.2 ± 0.6	4.9 ± 0.7	7.3 ± 0.1	5.1 ± 0.3
Live branches		2.6 ± 0.9	5.6 ± 1.4	7.6 ± 0.4	5.7 ± 1.2	6.7 ± 0.9	9.8 ± 0.1	6.9 ± 0.6
Dead branches and needles		0.1 ± 0.1	1.4 ± 0.9	3.5 ± 0.5	9.7 ± 3.1	10.7 ± 1.5	7.5 ± 0.5	8.6 ± 2.1
Aboveground biomass	1.7 ± 0.3†	7.9 ± 3.4	26.8 ± 9.9	44.2 ± 3.0	93.8 ± 20.9	118.2 ± 16.9	176.5 ± 3.9	126.4 ± 10.9
Coarse roots (>5 mm)		2.9 ± 1.3	9.3 ± 3.1	14.6 ± 0.8	20.2 ± 4.3	23.9 ±.3.3	34.0 ± 0.6	24.6 ± 2.4
Fine roots (<5 mm)‡		3.4 ± 1.5	n.d.	4.1 ± 1.3	n.d.	4.6 ± 1.9	0.6 ± 0.2	n.d.
Belowground biomass	0.6 ± 0.2†	6.3 ± 2.0	9.3 ± 3.1	18.7 ± 1.5	20.2 ± 4.3	28.5 ± 3.8	34.6 ± 0.6	24.6 ± 2.4
Litter	3.6 ± 1.2	5.3 ± 2.4	n.d.	10.1 ± 3.8	n.d.	18.2 ± 6.4	8.6 ± 5.3	20.5 ± 19.3
Harvest residue§		0	0	0	4.9 ± 2.9	26.7 ± 3.8	26.7 ± 4.9	n.d.
Soils (SOM)	97.2 ± 27.3	117.4 ± 23.7	n.d.	137.3 ± 55.7	n.d.	104.3 ± 37.7	102.1 ± 31.2	205.2 ± 133.6

Values are means ± standard deviations ($P < 0.05$, $n = 4$ plots per site).
n.d. = not determined.

* Stand age was normalized for YC 22 based on top height to age functions (Edwards and Christie, 1981).

† Non-forest biomass was primarily grassland.

‡ Fine root data were taken from Saiz *et al.* (2006).

§ The harvest residue includes brash, stump, root and coarse woody debris left on-site after harvest, taken from Tobin *et al.* (2007). The combined standard deviation (σ) for belowground biomass values = $\sqrt{(\sigma n_1^2 + n_2^2 + n_3^2 \cdots)}$.

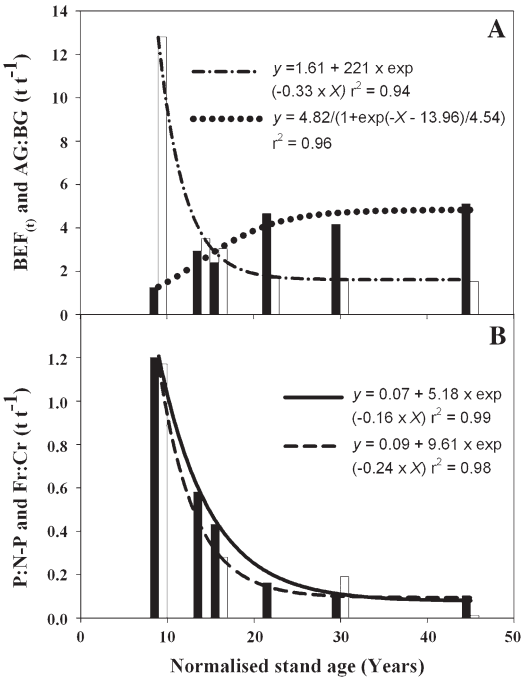

Figure 1. Changes in biomass allocation expressed in (A) BEF shown as the clear histogram and above to belowground ratio (AG : BG) shown as black histogram and in (B) the photosynthetic (live branches and needles) to non-photosynthetic biomass ratio (P : N-P) shown as the black histogram and the fine root to coarse root ratio (Fr : Cr) shown as the clear histogram. Regression lines are included only to indicate the allocation patterns over the first rotation (r^2 is the coefficient of correlation and X is normalized stand age).

relative to the non-photosynthetic (i.e. stemwood, attached dead branches and needles), biomass pool (P : N-P, Figure 1B) decreased exponentially with age. These trends in the allocation into photosynthetic tissue were similar to the observed changes in the fine root (Fr) to coarse root (Cr) biomass ratio (Figure 1B). The coarse root biomass (Cr) initially increased and remained relatively constant at 20–30 t C ha^{-1} after canopy closure. Fine root biomass was relatively constant (~4 t C ha^{-1}) for most stands, with the exception of the stand at site D45, where the fine root biomass pool decreased sixfold. This may be associated with the different texture of the soil and topography at the C45 stand (Tables 3 and 5).

Soil and litter C stocks

Litter depth and C stocks increased with an increase in stand age and associated increases in LAI, harvest residue and stand biomass (Tables 2 and 5). In the 9-year-old site (D9), there was still living understorey vegetation and an open canopy, which partially explains the lower litter accumulation at this site. The oldest site (D47) showed greatest variation in litter accumulation due, in part, to standing water and patches of bare soil where no litter accumulated (Table 5). The accumulation of litter at the 45-year-old site (C45) was lower, when compared with the 47-year-old site (D47). However, the topography of this site (C45) was sloped with a gradient of 10 per cent. In addition, the soils from the C45 site had higher sand and lower clay contents (Table 3).

Afforestation resulted in an initial increase in soil C stock (in the bulked top 30-cm mineral layer, i.e. O, A, B and E horizons) from 97.2 ± 27.3 t C ha^{-1} in the unplanted grassland to 137.3 ± 55.7 t C ha^{-1} for the closed canopy stand (D14, Table 5). This represents an annual increment (ΔSOM) of 2.2–2.5 t C ha^{-1} year^{-1} over the first 16 years of the rotation. The ΔSOM decreased to 0.2 t C ha^{-1} year^{-1} in two of the older stands (D30 and C45, Figure 5). Again this lower accumulation of soil C in these older stands may be associated with the sloping topography in these stands (Table 3).

Net primary productivity

Stand and component NPP were estimated using biometric assessments from repeat inventories in 2002 and 2004 and biomass algorithms (see Table 6). Fine root growth (ΔFr) was taken from previously published papers (Saiz *et al.*, 2006; Black *et al.*, 2007). Where ΔFr and biomass detritus in the form of litter (ΔF_{litter}) was not determined (ages 14–16 and 22–24 years old), the mean component NPP across all stands was used (see footnote ¶ in Table 6).

Stand NPP was highest at canopy closure followed by a decline after the first thinning cycle (Figure 2). There was also a significant ($P < 0.01$) linear correlation between LAI and stand NPP over the chronosequence (inset of Figure 2, Tables 2 and 6).

Table 6: NPP of different biomass components over the chronosequence

	Stand age (years)*					
	9–11	14–16	16–18	22–24	30–32	45–47
NPP (t C ha^{-1} year^{-1})						
Stems	2.2 ± 1.1	8.4 ± 2.6	7.8 ± 0.9	7.8 ± 2.7	6.1 ± 1.1	5.2 ± 0.6
Timber	1.4 ± 0.9	7.9 ± 3.0	7.7 ± 0.8	7.0 ± 2.4	5.3 ± 0.9	4.6 ± 0.5
Needles	0.7 ± 0.2	0.7 ± 0.2	0.3 < 0.1	0.2 < 0.1	0.2 < 0.1	0.2 < 0.1
Live branches	0.9 ± 0.2	0.9 ± 0.3	0.4 < 0.1	0.4 ± 0.1	0.3 < 0.1	0.3 < 0.1
Attached dead branches	0.2 ± 0.2	1.5 ± 0.6	1.5 ± 0.2	0.5 ± 0.1	0.1 < 0.1	0.1 ± 0.1
Aboveground biomass†	3.9 ± 1.7	11.5 ± 2.7	10.1 ± 1.1	8.9 ± 3.1	6.8 ± 1.2	5.6 ± 0.1
Belowground biomass‡	1.4 ± 0.6	3.1 ± 0.3	2.4 ± 0.3	1.4 ± 0.5	1.1 ± 0.2	1.1 ± 0.2
Litter fall (ΔF_{litter})§	0.11 ± 0.02	0.14 ± 0.03	0.19 ± 0.03	0.14 ± 0.03	0.13 ± 0.02	0.12 ± 0.04
Fine root growth (ΔFr)	0.38 ± 0.11¶	0.35 ± 0.09#	0.43 ± 0.18¶	0.35 ± 0.09#	0.41 ± 0.05¶	0.16 ± 0.04¶
NPP‖	5.79 ± 1.81	15.09 ± 2.71	13.12 ± 1.15	10.76 ± 3.14	8.44 ± 1.23	6.98 ± 0.23

NPP is expressed as current annual increment based on survey data taken in 2002 and 2004. Values are means ± standard deviations ($P < 0.05$, $n = 4$ plots per site).

* Stand age was normalized for YC 22 based on top height–age functions ((Edwards and Christie, 1981).

† aboveground biomass = total biomass – coarse root biomass.

‡ belowground biomass only includes coarse roots (>5 mm).

§ current year litter only include green shoots and bud scales.

¶ fine root growth was taken from Black *et al.* (2007) and Saiz *et al.* (2006).

where fine root data were not determined, the mean value for all sites was used.

‖ NPP = DB (aboveground + belowground NPP) + ΔF_{litter} + ΔFr (see Black *et al.*, 2007).

Aboveground biomass increment represented the largest component of stand NPP, accounting for 68–81 per cent of the NPP stock increment (Table 6). Timber NPP (current annual increment of timber biomass) varied from 1.4 to 7.7 t C ha^{-1} year^{-1} and was highest at canopy closure and after the first thinning cycle. The equivalent volume increment at felling (i.e. at site C45 = 24 m^3 ha^{-1} year^{-1}) was broadly consistent with the Forestry Commission YC table predictions (YC = 22, see Table 2, Edwards and Christie, 1981). This is based on a wood basic density of 0.4 t m^{-3} and a C content of 49 per cent (Black *et al.*, 2006). Annual C storage in the photosynthetic tissue (needles and live branches) initially increased as the canopy developed, but subsequently declined due to needle senescence (site D14), thinning operations and a higher allocation into timber and dead branch biomass (Table 6).

Changes in coarse root belowground NPP over the chronosequence were similar to the trends observed for NPP of photosynthetic tissue. However, the NPP of fine roots (ΔFr) was constant across the chronosequence.

The loss of live needles, shoots and buds from the aboveground component, as litter (ΔF_{litter}), did not vary across the chronosequence and was only ~3 to 5 per cent of total litter fall.

Gross primary productivity

There was generally a good agreement (($r^2 = 0.72$), $P < 0.001$; slope = 1.02 and root mean squared error (RMSE) = 1.8) between the MAESTRA-based and eddy covariance-based estimates of daily GPP (Figure 3). Estimates of GPP for three other stands (B9, D30 and C45) were simulated using the same physiological parameters as those used for the D14 stand. Although we could not validate the GPP predictions for the other stands across the chronosequence, we assumed that there were no systematic under- or overestimation of GPP in the different aged stands.

The age-related trends in GPP mirrored those observed for NPP and LAI (Figures 2 and 4). Stand GPP initially increased as the canopy closed, followed by a decline due to the removal of photosynthetic tissue during thinning operations.

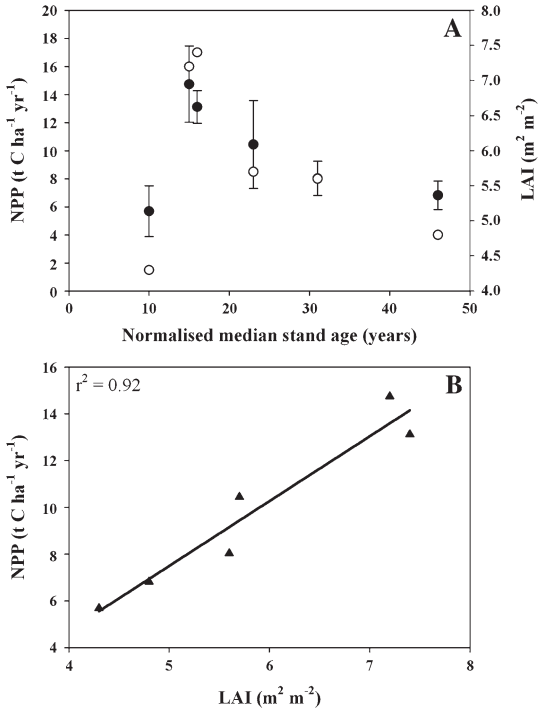

Figure 2. (A) Age-related changes in LAI (shown as the white circles) and NPP (shown as black circles with standard error bars) over the Sitka spruce chronosequence; (B) the linear relationship between LAI and NPP (black triangles).

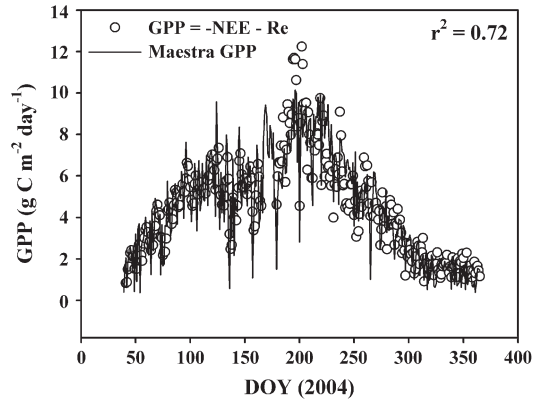

Figure 3. Cross-validation of GPP estimates based on the MAESTRA model (solid line) and eddy covariance measurements (white circles) for the core site (D14) in 2003. The correlation between coefficient modelled and measured GPP estimates were significant at $P < 0.001$; slope = 1.02 and RMSE = 1.8.

Integration of chronosequence data

The chronosequence approach, together with modelling and flux measurements, shows that afforested stands are a C sink after 10 years, and possibly earlier, followed by a further increase to a maximum of 8–9 t C ha^{-1} year^{-1} before the first thinning cycle (Figure 4). There was good agreement between the inventory/modelling (equation 2) and eddy covariance-based estimates of NEP at the reference stand (D14, Figure 4). It was also possible, in most cases, to close the C balance for the sites investigated. However, there were some discrepancies in the C balance of the youngest stand, as evident from the higher root Ra when compared with the total ecosystem Ra (Ra = GPP − NPP).

The ratio of NPP to GPP, which represents the relative respiratory cost for forest growth, was 0.57, 0.69, 0.60 and 0.61 for the 9-, 16-, 30- and 45-year-old stands, respectively. The ratio of NEP to NPP, which reflects the relative heterotrophic respiratory (Rh) loss from soils, litter and harvest residue, was 0.24, 0.75, 0.42 and 0.30 for the 9-, 16-, 30- and 45-year-old stands, respectively. The lower NEP : NPP ratio in the youngest stand was primarily due to the relatively higher soil Rh, which may have been exacerbated by grassland root turnover and associated decomposition processes. The higher decomposition losses from the older stands were due to C losses associated with harvest residues (Hr, Figure 4).

Total belowground C allocation

The belowground inputs defined as litter and photoassimilates (photoassimilate input = TBCA − ΔLitter) were higher in the younger 9- and 16-year-old stands. Based on the TBCA and GPP estimates for the 16-, 30- and 45-year-old-stands, we estimate that 10–29 per cent of GPP is allocated to belowground processes.

The higher accumulation of soil C (ΔSOM) in younger, compared with older, stands was associated with a higher input of C, from litter, non-forest vegetation and photoassimilates, and a relatively higher C loss via heterotrophic respiration from soils (Figure 5). This is consistent with the decrease in the ratio of TBCA : $Fs_{(het)}$ from ~2.8, in the younger stands, to 1.6 in the older stands. Total soil respiratory losses were greater than the TBCA in the 30- and 45-year-old stands

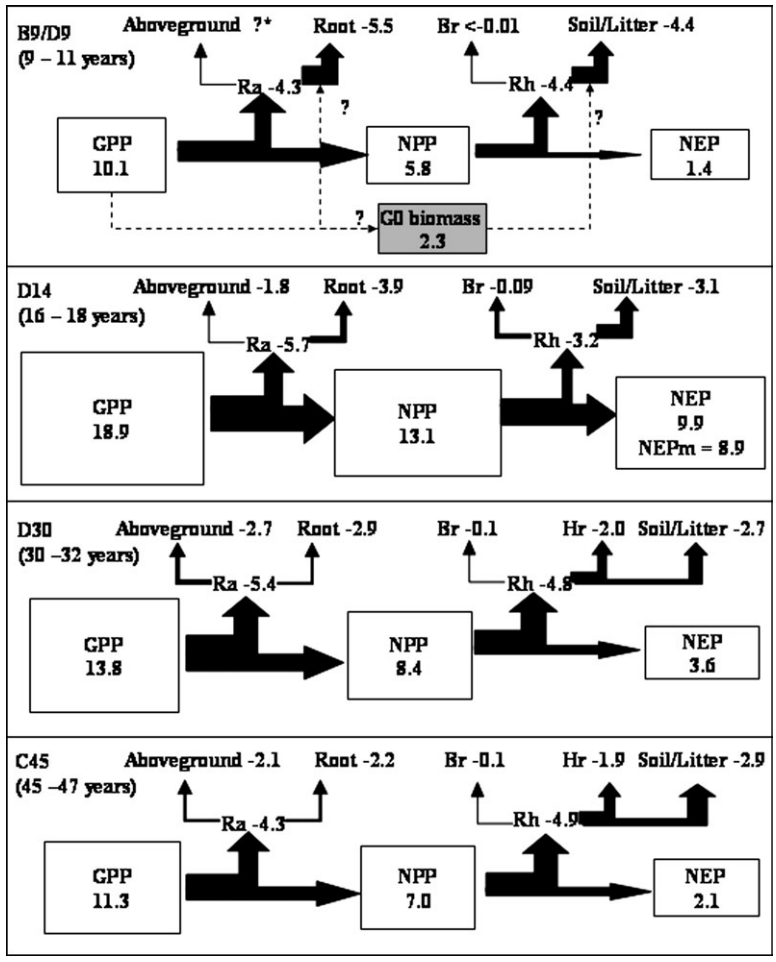

Figure 4. Age-related changes in ecosystem and component C fluxes across the Sitka spruce chronosequence. Details relating to the different sites B9/D9, D14, D30 and C45 are listed in Tables 1–3. NEPm is eddy covariance-derived net ecosystem exchange (Black *et al.*, 2007) and NEP, net ecosystem exchange (see test for description and derivation of fluxes). Negative flux values represent a loss of C (i.e. a C source) and positive values represent a C sink. It was not possible to close the C balance in the 9- to 11-year-old stand.

despite the small increase in ΔSOM. This may reflect the efflux of C from decomposing stumps and roots following thinning operations in older stands.

Discussion

The chronosequence approach is a useful tool to rapidly obtain information on age-related changes in ecosystem C balance over time (as shown in this study, Mund *et al.*, 2002; Zerva *et al.*, 2005). Our experimental, modelling and flux measurements show that it was, in most cases, possible to close the C balance for different aged stands. The failure to close the C balance in the 9- to 11-year-old stands (Figure 4) could arise from an underestimation of GPP and/or the omission of contributing fluxes from the grassland vegetation. Most process-based forest C balance models, including MAESTRA, do not simulate non-forest vegetation C dynamics. For the purpose of this exercise, grassland NEP

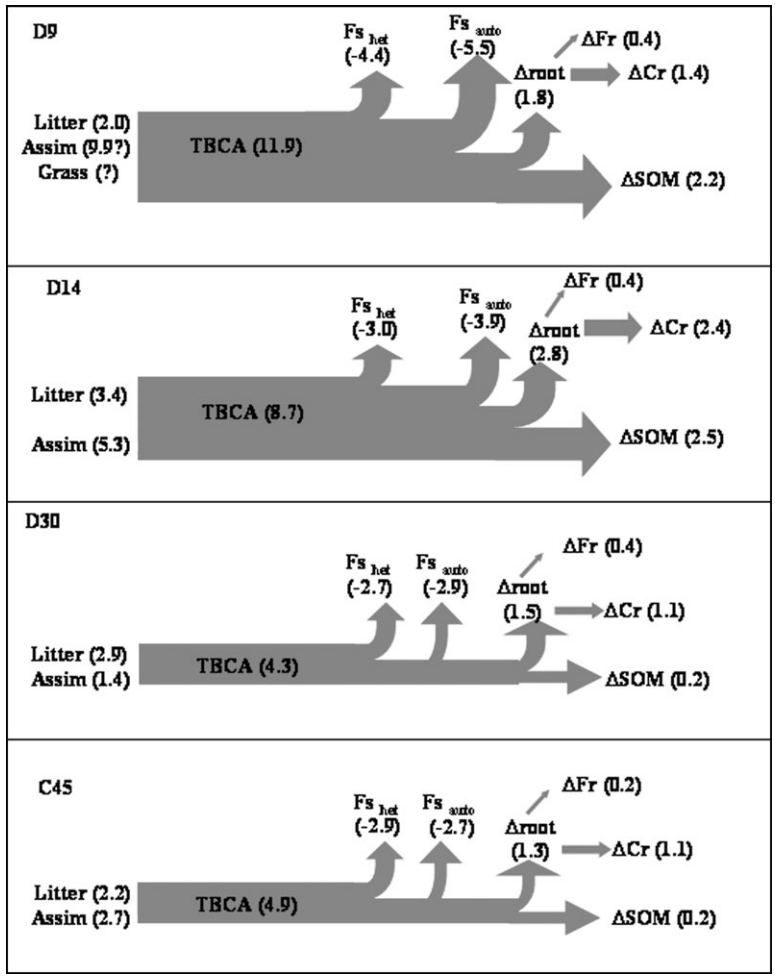

Figure 5. Age-related changes in TBCA and component fluxes across the Sitka spruce chronosequence. Details relating to the different aged stands are listed in Tables 1–3. Assim., photoassimilates; Fs_{het}, heterotrophic soil respiration; Fs_{auto}, autotrophic soil respiration; Δroot, total root turnover; ΔFr, fine root turnover; ΔCr, coarse root turnover and ΔSOM, change in soil C stocks (see text for description and derivation of fluxes).

was assumed to be zero. The high root Ra rate measured at the 9-year-old stand (Saiz *et al.*, 2006) could also include C efflux from non-forest vegetation. It is plausible that total ecosystem GPP and NPP fluxes (i.e. forest and non-forest vegetation) for the 9-year-old stand could be larger and NEP fluxes either larger or smaller if grassland dynamics relating to the transition to forestry were included. The non-forest vegetation dynamics following land use transition into forests is an important pool required for reporting forest sources and sinks under article 3.3 of the Kyoto protocol. Ecosystem flux measurements across a Sitka spruce chronosequence on deep blanket peat in Scotland suggests that C losses following afforestation are compensated for by the rapid uptake of C by non-forest vegetation (Hargreaves *et al.*, 2003). In contrast, the contribution of non-forest vegetation to the C balance in the older stands is very small and it can be assumed that the contribution to ecosystem C balance in Sitka spruce stands, following canopy closure, is negligible (Black *et al.*, 2007).

The results presented here show that afforested stands are a C sink at 10 years, and possibly earlier, followed by an increase to a maximum of 9 t C ha^{-1} $year^{-1}$ before the first thinning cycle. NEP subsequently declined from 9 t C ha^{-1} $year^{-1}$, at closed canopy, to ~2 t C ha^{-1} $year^{-1}$ in older, thinned stands. These findings are consistent with ecosystem flux measurements reported for Sitka spruce stands in the UK, which varied from 7 t C ha^{-1} $year^{-1}$ at canopy closure to 3 t C ha^{-1} $year^{-1}$ in older stands (Kowalski *et al.*, 2004; Magnani *et al.*, 2007). However, the maximum NEP of Sitka spruce stands, as determined by eddy covariance (this study; Kowalski *et al.*, 2004), were higher than the values reported (0.2–6.5 t C ha^{-1} $year^{-1}$) for other coniferous forest stands across Europe (Magnani *et al.*, 2007). These findings support a previous suggestion that Sitka spruce plantations in Ireland and the UK may be the species of choice for realizing the maximum C sequestration potential (Dewar and Cannell, 1992).

A comparison of ecosystem and component C fluxes obtained from this study and data for other temperate coniferous forests from European and global databases (see Luyssaert *et al.*, 2007; Magnani *et al.*, 2007) suggest that the high sequestration potential of Sitka spruce on surface-water gley soils is possibly associated with a proportionally lower respiratory loss (Zerva *et al.*, 2005). This is illustrated by the lower mean Ra : GPP (0.67) ratios for the closed C balance stands (Figure 4), when compared with other published values (0.76–0.82) for coniferous forests in temperate regions (Luyssaert *et al.*, 2007; Magnani *et al.*, 2007). The higher mean NPP : GPP ratio (0.63) presented here, compared with other published mean values (0.44) for temperate conifer forests (Luyssaert *et al.*, 2007), suggests that maintenance and growth respiration in intensively managed Sitka spruce plantations are lower than other conifer forests. This may be due to a higher LAI and increased allocation into photosynthetic biomass, when compared with other temperate forest plantation species (see Luyssaert *et al.* 2007). The mild oceanic climate with a higher rainfall and relative humidity in Ireland (Hemming *et al.*, 2005; Black *et al.*, 2007) may facilitate a higher LAI, NPP, NEP and lower respiratory losses, when compared with other European forests (Hemming *et al.*, 2005; Luyssaert *et al.*, 2007).

An alternative explanation for variations in NEP and Rd : GPP ratio across different temperate conifer forests may be coupled to age-related changes in NEP, GPP and Ra. The stands listed in several comparative studies (0–120 years old, see Hemming *et al.*, 2005; Luyssaert *et al.*, 2007; Magnani *et al.*, 2007) are generally older than those reported in this study (Table 1). While it has been suggested that the ratios of NPP : GPP are relatively constant across various forest types (Waring *et al.*, 1998; Luyssaert *et al.*, 2007), other studies (Mäkelä and Valentine, 2001) suggest that NPP : GPP could vary with stand age (Figure 4). We suggest that age-related decline in NEP in older stands in this study may be due to three major factors: (1) a decrease in GPP; (2) an increase in maintenance and growth respiration (i.e. a lower NPP : GPP) and (3) an increase in decomposition losses following disturbance (i.e. a lower NEP : NPP). A reduction in GPP in older stands may primarily be due to thinning and canopy senescence, which effectively reduces the LAI and light capture by the stand (Chapin *et al.*, 2002). Light capture is further reduced by an increased allocation of C into non-photosynthetic material, such as timber (Figure 1). It has also been suggested that hydraulic constants also limit GPP in older stands (Mencuccini and Grace, 1996). The hydraulic limitations on GPP have not, however, been characterized in MAESTRA. Age-related variations in NPP : GPP following canopy closure have been related to an increase in maintenance respiration (Mäkelä and Valentine, 2001), a component of Ra. We suggest that this may be associated with a higher allocation of biomass into non-photosynthetic tissue (Figure 1). The fluctuations in NEP across the age sequence were also associated with alternations in NEP : NPP, which reflects differences in the relative decomposition losses. Management-related disturbance events, such as establishment and thinning, result in an increase in decomposition losses from forest stands (Figure 4; Chapin *et al.*, 2002; Kolari *et al.*, 2004).

The long-term storage of C in forest ecosystems is a function of allocation and sequestration of biomass C into soils. In this study we show that land use change from unmanaged grasslands to Sitka spruce forests on wet mineral gley soils resulted in an accumulation of soil C (in the top 30 cm) over the first rotation. In a similar study conducted on peaty gley soils, it was shown that ~100 t C was lost from these soils following afforestation of grassland with Sitka spruce (Zerva *et al.*, 2005). The estimated TBCA values presented in this study are

within the global range of 2.6–11.3 t C ha^{-1} $year^{-1}$ presented by Raich and Nadelhoffer (1989) as well as values reported by Zerva *et al.* (2005). Comparisons of TBCA and GPP values, obtained from eddy covariance measurements and MEASTRA model predictions, showed that 31–43 per cent of GPP is allocated to belowground pools in the 16- to 45-year-old stands (Figures 4 and 5). These values are consistent with previous estimates (31 and 57 per cent) for Sitka spruce in the UK. (Zerva *et al.*, 2005). The accumulation of C in wet mineral gley soils may be associated with the higher TBCA and reduced decomposition due to anaerobic conditions normally associated with these water-saturated soils. The TBCA previously reported for a mature Sitka spruce afforested stand on peaty gley soils was 1 t C ha^{-1} $year^{-1}$ (Zerva *et al.*, 2005) compared with 4.9 C ha^{-1} $year^{-1}$ for a mature afforested stand located on a surface-water gley in the present study (Figure 5). The higher TBCA reported for stands investigated in this study were associated with higher litter inputs, consistent with the differences in YC between the two stands (10–12 in the UK *vs* 22–24 in Ireland). In addition, the turnover and loss of these belowground pools in mature afforested Sitka spruce stands, measured as total soil respiration (~5 t C ha^{-1} $year^{-1}$), was similar for both the peaty gley (Zerva *et al.*, 2005) and surface-water gley soils (Saiz *et al.*, 2006, Figure 5). While belowground component fluxes in young afforested peaty gley soils were not reported by Zerva *et al.* (2005), is it plausible that creation of aerobic conditions in the peat layer following afforestation would have resulted in a significant loss of labile soil C (Zerva *et al.*, 2005). Other peat land C flux studies suggest the loss of soil C from afforested peat soils is initially rapid followed by a slower release after 4–8 years (Hargreaves *et al.*, 2003). Slower peat decomposition in older stands (e.g. reported by Zerva *et al.*, 2005) may be due to inhibition of decomposition associated with a lower pH, decreased soil temperature due to shading or reduced litter quality (Hargreaves *et al.*, 2003).

Although the age sequence of stands was selected to minimize constraints associated with differences in ecological conditions, silviculture and land use history, these constraints could not be completely satisfied simultaneously. It was particularly difficult to select an identical soil type across the chronosequence within a similar geographic location representing a similar previous land use. Sites represented by a sloping topography were characterized by a more sandy soil, with a lower moisture content. The results presented in this and associated studies (Saiz *et al.*, 2006, 2007) suggest that site topography can influence the fine root turnover, soil and litter C accumulation. It is also plausible that the lower soil moisture content at D30 and C45 stands (Saiz *et al.*, 2006) may result in a higher turnover and decomposition of litter and root exudates in the older stands in the chronosequence.

Funding

The Irish National Council for Forest Research and Development to CARBiFOR I project (2002–2006).

Acknowledgements

The authors are grateful for assistance rendered by Marie Mannion, John O'Brien, Sean Caplice and Paddy Fitzgerald of Coillte for providing maps, inventory and management details of the sites surveyed.

Conflict of Interest Statement

None declared.

References

Black, K., Tobin, B., Saiz, G., Byrne, K. and Osborne, B. 2004 Improved estimates of biomass expansion factors for Sitka spruce. *J. Ir. For.* **61**, 50–65.

Black, K., Davis, P., Mc Grath, J., Doherty, P. and Osborne, B. 2005 Interactive effects of irradiance and water availability on the photosynthetic performance of *Picea sitchensis* seedlings: implications for seedling establishment under different management practices. *Ann. For. Sci.* **62**, 413–422.

Black, K.G., Davis, P., Lynch, P., Jones, M., McGettigan, M. and Osborne, B. 2006 Long-term changes in solar irradiance in Ireland and their potential effects on gross primary productivity. *Agric. For. Meteorol.* **141**, 118–132.

Black, K.G. and Farrell, E.P. (eds). 2006 *Carbon Sequestration in Irish Forest Ecosystems*. Council for Forest Research and Development (COFORD), Dublin, p 76.

Black, K.G., Bolger, T. and Davis, P. *et al.* 2007 Inventory and eddy covariance based estimates of annual carbon sequestration in a Sitka spruce (*Picea sitchensis* (Bong.) Carr.) forest ecosystem. *J. Eur. For. Res.* **126**, 167–178.

Chapin, S.S., Matson, P.A. and Mooney, H.A. 2002 *Principles of Terrestrial Ecosystem Ecology*. Springer, New York, pp. 97–122.

Dewar, R.C. and Cannell, M.G.R. 1992 Carbon sequestration in trees, products and soils of forest plantations: an analysis using UK examples. *Tree Physiol.* **11**, 49–71.

Edwards, P.N. and Christie, J.M. 1981 *Yield Models for Forest Management*. Forestry Commission Booklet No. 48. HMSO, London.

Giardina, C.P. and Ryan, M.G. 2002 Total belowground carbon allocation in a fast growing *Eucalyptus* plantation estimated using the carbon budget approach. *Ecosystems*. **5**, 487–499.

Hargreaves, K.J., Milne, R. and Cannell, M.G.R. 2003 Carbon balance of afforested peatland in Scotland. *Forestry*. **76**, 299–317.

Hemming, D., Yakir, D. and Ambus, P. *et al.* 2005 Pan-European δ13C values of air and organic matter from forest ecosystems. *Global Change Biol.* **11**, 1065–1101.

Kolari, P., Pumpanen, J., Rannik, Ü, Ilvesniemi, H., Hari, P. and Berninger, F. 2004 Carbon balance of different aged Scots pine forests in Southern Finland. *Global Change Biol.* **10**, 1–14.

Kowalski, A.S., Loustau, D. and Berbigier, P. *et al.* 2004 Paired comparisons of carbon exchange between undisturbed and regenerating stands in four managed forests in Europe. *Global Change Biol.* **10**, 1707–1723.

Luyssaert, S., Inglima, I. and Jung, M. *et al.* 2007 The CO_2-balance of boreal, temperate and tropical forests. *Global Change Biol.* **13**, 1–29.

Magnani, F., Mencuccini, M. and Borghetti, M. *et al.* 2007 The human footprint in the carbon cycle of temperate and boreal forests. *Nature*. **447**, 848–852.

Mäkelä, A. and Valentine, H.T. 2001 The ratio of NPP to GPP: evidence of change over the course of stand development. *Tree Physiol.* **21**, 1015–1030.

Medlyn, B.E. and Jarvis, P.G. 1999 Design and use of a database of model parameters from elevated [CO_2] experiments. *Ecol. Modell.* **124**, 69–83.

Mencuccini, M. and Grace, J. 1996 Hydraulic conductance, light inception and needle nutrient concentration in Scots pine stands and their relation with net primary productivity. *Tree Physiol.* **16**, 459–468.

Mund, M., Kummetz, E., Hein, M., Bauer, G.A. and Schulze, E.-D. 2002 Growth and carbon stocks of a spruce forest chronosequence in central Europe. *For. Ecol. Manage.* **171**, 275–296.

Norman, J.M. and Jarvis, P.G. 1974 Photosynthesis in Sitka spruce (*Picea sitchensis* (Bong.) Carr.) III. Measurements of canopy structure and interception of radiation. *J. Appl. Ecol.* **11**, 375–398.

Norman, J.M. and Jarvis, P.G. 1975 Photosynthesis in Sitka spruce (*Picea sitchensis* (Bong.) Carr.): V. Radiation penetration theory and a test case. *J. Appl. Ecol.* **12**, 839–878.

Raich, J.W. and Nadelhoffer, K.J. 1989 Belowground carbon allocation in forest ecosystems: global trends. *Ecology*. **70**, 1346–1354.

Saiz, G., Byrne, K.A., Butterbach-Bahl, K., Kiese, R., Blujdea, V. and Farrell, E.P. 2006 Stand age-related effects on soil respiration in a first rotation Sitka spruce chronosequence in central Ireland. *Global Change Biol.* **12**, 1007–1020.

Saiz, G., Black, K., Reidy, B., Lopez, S. and Farrell, E.P. 2007 Assessment of soil CO2 efflux and its components using a process-based model in a young temperate forest site. *Geoderma*. **139**, 79–89.

Sims, P.L., Singh, J.S. and Lauenroth, W.K. 1978 The structure and function of ten Western North American grasslands. *J. Ecol.* **66**, 251–285.

Tobin, B., Black, K., Osborne, B., Reidy, B., Bolger, T. and Nieuwenhuis, M. 2006 Assessment of allometric algorithms for estimating leaf biomass, leaf area index and litter fall in different aged Sitka spruce forests. *Forestry*. **79**, 453–465.

Tobin, B., Black, K., McGurdey, L. and Nieuwenhuis, M. 2007 Towards a methodology for assessing carbon stock changes in coarse woody debris. *Forestry*. **80**, 455–469.

Wang, Y.P. and Jarvis, P.G. 1990a Influence of crown structural properties on PAR absorption, photosynthesis, and transpiration in Sitka spruce—application of a model (MAESTRO). *Tree Physiol.* **7**, 297–316.

Wang, Y.P. and Jarvis, P.G. 1990b Effect of incident beam and diffuse radiation on PAR absorption, photosynthesis and transpiration of Sitka spruce—a simulation study. *Silva Carelica*. **15**, 167–180.

Wang, Y.P. and Jarvis, P.G. 1993 Influence of shoot structure on the photosynthesis of Sitka spruce (*Picea sitchensis*). *Funct. Ecol.* **7**, 433–451.

Waring, R.H., Landsberg, J.J. and Williams, M. 1998 Net primary production of forests: a constant fraction of gross primary production? *Tree Physiol.* **18**, 129–134.

Zerva, A., Ball, T., Smith, K.A. and Mencuccini, M. 2005 Soil carbon dynamics in a Sitka spruce (*Picea sitchensis* (Bong.) Carr.) chronosequence on a peaty gley. *For. Ecol. Manage.* **205**, 227–240.

Received 17 December 2007

Appendix 1

Parameters, settings, values and sources used to run MAESTRA

Parameter	Description	Value	Notes/source
Control files	Confile.dat		
IOHOURLY	Hour counter for simulation	0	Daily output
IOTUTD	Controls how often diffuse fractions are calculated	1	Once a day
IORESP	Simulation of respiration fluxes	1	Daily output
START	Start date for simulation	1 January 2002	
END	End date for simulation	31 December 2002	
NSTEP	Calculation outputs	1	Daily output
NOTREES	Number of trees in plot	50	Based on survey (this study)
NOTARGET	Number of target trees used when calculating radiation interception	10–20	Based on survey (this study)
NOLAY	Number of canopy layer used to calculate interception	6	Default
NZEN	Number of zenith angles to calculate diffuse transmittance	5	Default
NAZ	Number of azimuth angles to calculate diffuse transmittance	11	Default
MODELGS	Stomatal conductance model	1	Wang and Jarvis (1990b)
MODELJM	Farquhar parameters	1	From N content file
MODELRD	Leaf respiration model	1	From N content file
MODELSS	Wood respiration model	0	Depends on woody biomass
MODELSS	Calculation of sun/shade leaves	0	Average PAR
ITERMAX	Photosynthesis/transpiration	0	Use leaf temperature
OIHIST	PAR histogram	0	No output
Tree files	trees.dat		
X,YMAX	Plot dimension (m)	*	See survey methods
SLOPE	Slope in XY	*	See Table 2
XYCOORDS	x–y coordinates for each tree	Variable	Measured in ploy surveys
ALLRAD	Crown radius in X and Y	*	See survey methods
ALLHTCROWN	Crown height	*	Survey (Table 2)
ALLDIAM	d.b.h.		Survey (Table 2)
ALLAREA	Area per tree	*	Appendix B
PHENOLOGY	Area development	0	Assumed to be negligible
Climate files	met.dat		
DAYORHR	Daily or hourly output	1	Daily
CA	Ambient CO_2 concentration	380ppm	From eddy covariance (site D14)
DIFSKY	Distribution of diffuse radiation	0	Uniform
PRESS	Atmospheric pressure (Pa)	†	Form met station
WIND	Wind speed above canopy (m s^{-1})	†	Form met station
TMIN	Minimum temperature (°C)	†	Form met station
TMAX	Minimum temperature (°C)	†	Form met station
PAR	(400–700 nm, MJ d^{-1})	†	Form met station
SI	Shortwave incident radiation	*	Norman and Jarvis (1975)
FBEAM	Direct beam PAR fraction	*	Norman and Jarvis (1975)
LAT	Latitude	*	See Table 1
LONHEM	Hemisphere	W	

Appendix 1: *continued.*

Parameter	Description	Value	Notes/source
LATHEM	Hemisphere	N	
LON	Longitude	*	See Table 1
TZLONG	Longitude of the meridian time zone	0	
Crown Structure	Str.dat		
CSHAPE	Crown shape	CONE	
ELP	Leaf angle distribution	1	Spherical (Wang and Jarvis, 1990b)
NALPHA	Number of leaf age classes	1	Default value
JLEAF	Leaf area density distribution	2	Beta distribution (Wang and Jarvis, 1990b)
BPT	Beta distribution coefficients	Variable	(Norman and Jarvis, 1974; Wang and Jarvis, 1990b)
RANDOM	Clumping factor	0.7	Norman and Jarvis (1974), projected to shoot to needle ratio
NOAGEC	Number of age classes for which leaf area distribution is specified	1	
NFOL	Seasonal variation in leaf N	0	No variation
EXTWIND	Decline in wind speed in canopy	0	Default
COEFFT	Allometric coefficient for woody biomass	102.08	‡
EXPONT	Allometric coefficient for woody biomass	1.687	‡
BCOEFFT	Allometric coefficient for branch biomass	2.28	‡
BEXPONT	Allometric coefficient for branch biomass	0.686	‡
RCOEFFT	Allometric coefficient for roots	11.66	‡
REXPONT	Allometric coefficient for roots	0.99	‡
FRFARC	Fine root fraction of total root	0.3	This study (assumed to be constant in MAESTRA)
Physiological parameters	phy.dat		
NOAGEP	Number of age classes for which physiological parameters are specified	1	
NOLAYERS	Number of layers for which reflectance and transmittance are specified	1	
RHSOIL	Soil reflectance (PAR, NIR, thermal)	0.1 0.3 0.05	Norman and Jarvis (1974)
ATAY	Leaf transmittance (PAR, NIR, thermal)	0.03 0.26 0.01	Norman and Jarvis (1974)
ARHO	Leaf refectance (PAR, NIR, thermal)	0.09 0.33 0.05	Norman and Jarvis (1974)
JMAXA	Electron transport rate (*J*max μmol m^{-2} s^{-1})	71	Black *et al.* (2005)
JMAXB	Electron transport rate (*J*max μmol m^{-2} s^{-1})	−3	Black *et al.* (2005)
VMAXA	Carboxylation parameter (μmol m^{-2} s^{-1})	32	Black *et al.* (2005)
VMAXB	Carboxylation parameter (μmol m^{-2} s^{-1})	−2	Black *et al.* (2005)
THETA	Curvature of electron transport curve	0.8	Wang and Jarvis (1993)

Appendix 1: *continued*.

Parameter	Description	Value	Notes/source
EAVJ	Activation energy of *J*max (J mol^{-1} K^{-1})	37 000	Medlyn and Jarvis, 1999
EDVJ	Deactivation energy of *J*max (J mol^{-1} K^{-1})	220 000	Medlyn and Jarvis (1999)
DELSJ	Entropy term (J mol^{-1})	710	Medlyn and Jarvis (1999)
EVAC	Activation energy of *V*max (J mol^{-1} K^{-1})	58 520	Medlyn and Jarvis (1999)
EDVC	Curvature of temperature response to *Vc* (J mol^{-1})	0	Medlyn and Jarvis (1999)
DELSC	Curvature of temperature response to J (J mol^{-1})	0	Medlyn & Jarvis (1999)
RTEMP	Temperature at which RD is specified (°C)	25	Wang and Jarvis (1990a)
Q10F	Foliage temperature response exponent	0.083	Wang and Jarvis (1990a)
DAYRESP	Faction by which dark respiration in inhibited in the light	1	Medlyn and Jarvis (1999)
GSJA	Constant in linear response of stomatal conductance (mol μmol^{-1})	0.0004	Medlyn and Jarvis (1999)
RDA	Leaf dark respiration parameter (μmol m^{-2} s^{-1})	0.95	Black *et al.* (2005)
RDB	Leaf dark respiration parameter (μmol m^{-2} s^{-1})	−0.62	Black *et al.* 2005
GSREF	Maximal stomatal conductance (mmol m^{-2} s^{-1})	0.38	Black *et al.* (2005)
GSMIN	Cuticular conductance (mmol m^{-2} s^{-1})	0.003	Wang and Jarvis (1990a)
PAR0	Stomatal conductance irradiance response parameter	20	Wang and Jarvis (1990a)
D0	Stomatal conductance humidity response parameter	375	Wang and Jarvis (1990a)
T0	Minimum temperature at which conductance = GSMIN (°C)	−5	Wang and Jarvis (1990a)
TMAX	Maximum temperature at which conductance = GSMIN	40	Wang and Jarvis (1990b)
TREF	Temperature at which conductance = GSREF	15	Wang and Jarvis (1990b)
WLEAF	Needle width (m)	0.002	M. Mencuccini (unpublished data)
NSIDES	Number of sides of needle with stomata	1	M. Mencuccini (unpublished data)
EFFY	Coefficient of growth respiration for woody biomass (g g^{-1})	0.33	Medlyn and Jarvis (1999)
RMW	Woody, branch and root biomass maintenance respiration (g CO_2 g^{-1} DW)	0.08807	Medlyn and Jarvis (1999)
Q10W,B	Woody and branch biomass respiration response exponent	0.07	Medlyn and Jarvis (1999)
RTEMP	Room temperature at which RMW is specified (°C)	15	Medlyn and Jarvis (1999)
Q10R	Root biomass respiration response exponent	4.1	Saiz et al. (2006)*
SLA	Specific leaf area (m^2 kg^{-1})	4.46	Tobin et al (2006)*

NIR = near infra-red radiation; PAR = photosynthetically active radiation; RD = dark respiration; Var. = variable.
* Specific values for plots calculated or measured during surveys.
† All climatic variables obtained from met station installed at D16 site.
‡ Biomass algorithms form harvested trees in this study, but specifically derived for MAESTRA: BIOM = COEFFT × H × (d.b.h.^{EXPONT}) + INRERC, where INTERC = 0.